Structural Engineering and Mechanics, Vol. 40, No. 4 (2011) 563-581
DOI: http://dx.doi.org/10.12989/sem.2011.40.4.563

Stability analysis of bimodular pin-ended slender rod

Wenjuan Yao*, Jianwei Ma[a] and Baolin Hu[b]

Department of Civil Engineering, Shanghai University, Shanghai 200072, China

(Received October 12, 2010, Revised May 19, 2011, Accepted October 12, 2011)

Abstract. Many novel materials, developed in recent years, have obvious properties with different modulus of elasticity in tension and compression. The ratio of their tensile modulus to compressive modulus is as high as five times. Nowadays, it has become a new trend to study the mechanical properties of these bimodular materials. At the present stage, there are extensive studies related to the strength analysis of bimodular structures, but the investigation of the buckling stability problem of bimodular rods seems to cover new ground. In this article, a semi-analytical method is proposed to acquire the buckling critical load of bimodular slender rod. By introducing non-dimensional parameters, the position of neutral axis of the bimodular rod in the critical state can be determined. Then by combining the phased integration method, the deflection differential equation of bimodular pin-ended slender rod is deduced. In addition, the buckling critical load is obtained by solving this equation. An example, which is conducted by comparing the calculation results between the three of the methods including the laboratory tests, numerical simulation method and the method we developed here, shows that the method proposed in the present work is reliable to use. Furthermore, the influence of bimodular characteristics on the stability is discussed and analyzed.

Keywords: bimodular; slender rod; buckling critical load; semi-anlytical method; nondimensional parameters

1. Introduction

Numerous studies (Destrade *et al.* 2009, Barak *et al.* 2009, Klisch 2006, Bertoldi *et al.* 2008) have indicated that many materials exhibit a phenomenon that the elastic properties in the extension differ from those in the compression. This phenomenon known as bimodularity has been experimentally demonstrated in many engineering materials such as concrete, metal, graphite, plastic, rock, and biomaterials, etc. Especially for the new polymer materials and composite materials, which have been developed in recent years, the ratio of their tensile modulus to compression modulus is as high over four times. Therefore, great attention has been paid to the study on mechanical behaviors of structures of these bimodular materials.

The elastic theroy of different modulus was firstly proposed by Jones (1977), Bert (1977), American researcheres, and Ambartsumyan (1986), a Russian researcher. In 1986, Ambartsumyan published his monograph about the elasticity of different moduli. In his book, he summarized the

*Corresponding author, Professor, E-mail: wjyao@shu.edu.cn
[a]Master Student
[b]Ph.D.

initial concept of different tension-compression modulus, basic assumptions and presented a criterion to distinguish between the tensile zone and compressive zone based on the sign of the normal stress.

Owing to the constitutive discontinuity, analytical solutions are difficult to find in general, for the analysis of bimodular structures, the finite element method and iterative techniques were therefore exploited in numerical calculations (Tseng and Lee 1995, Ye 1997, Tseng and Jiang 1998, Yao *et al.* 2006). Considering some advanced compound materials that display high bimodular characteristics, Raffaele (2001) and Patel (2004) adopted the finite element procedure to analyze the stress and deformation of bimodular laminated composite plates based on the model proposed by Bert (1977). The finite element methods were also extended to the non-linear analysis of composite plates (Bruno *et al.* 1994) and thermal buckling of sandwich beams (Lan *et al.* 2003). The stress-strain relation of a composite plate and a sandwich beam are somewhat similar to that of a bimodular plate and a bimodular beam. However, the buckling behaviour can be substantially different because additional bending action can be developed in a bimodular structure as the neutral axis moves during the buckling process. Becasuse of the complicated nature of the bimodular buckling problem, Bert and Ko (1985) used the finite difference method to analyze the buckling behaviour for bimodular cantilever column. Due to some problems including unstable iteration and slow convergency in calculations, a newly form of shear modulus (He *et al.* 2009) are proposed to increase the rate of iteration and convergence. Yang *et al.* (2006, 2009) described the non-linear relationship of stress and strain by employing smoothing functions, which can avoid the judgement of sign of the normal stress, thus leading to a higher computing efficiency. Based on this, the initial stress finite element method and the neural network model are established.

In view of the peculiar nonlinear (bilinear or piecewise linear) characteristics for bimodular problems, analytical solutions are only available in some typical structures. Yao and Ye (2004, 2005, 2006, 2008) resorted to the flowing coordinate system and phased integration method to deduce the analytical solution of neutral axis, stress, strain and displacement for bending-compression column, bending beam subject to lateral force, retaining wall and bending-compression/tension memebers with different modulus under complex stress and subjected to the combined loadings. They also developed the iterative program combining with the phased integration method for calculating nonlinear internal force and thermal stresses in statically indeterminate structures with different moduli. In order to simplify the derived process, He *et al.* (2007) obtained the approximate elasticity solution of a bimodular beam and a bimodular bending-compression column by employing the equivalent section method. Based on the equivalent modulus of elasticity of analytical solution for bending-compression column (Yao and Ye 2004), Qu (2009) derived the analytical solution for the deflection of geocell with different tension and compression modulus. By applying the principle of strain invariant, Cai and Yu (2009) developed a new kind of constitutive relation in the form of tensor for the elastic isotropy materials with different elastic moduli in tension and compression. Leal *et al.* (2009) derived the compressive strength equation of the high performance fibres with different modulus and analyzed the effects of bimodularity on the compressive strength.

The previous studies on the bimodular structures mainly focus on the strength analysis, whereas investigations of stability problem of bimodular structures or rods are scant. There are only very few computational methods for buckling behaviour of bimodular structures, which are actually derived from numerical methods. However, the numerical methods are complicated and time-consuming. The major obstacle of solving these bimodualr problems is caused by the nonlinear problems that the position of neutral axis in the buckling critical state is relative to both the critical load and critical deflection equation. With the above consideration, in this paper, a semi-analytical method is proposed to determine the position of the neutral axis in critical state by using the nondimensional parameters. Then the differential deflection equation of bimodular pin-ended slender rod is derived based on the phased integration method and the critical load is obtained. Finally, the effects of bimodular characteristics on the stability of bimodular rod are investigated.

2. Basic concept and assumption

In the action of tension or compression stress with the same absolute value, bimodular materials will produce a corresponding tension or compression strain with different absolute value. When this kind of materials are subjected to axial stress, the constitutive relationship of which is nonlinear (bilinear). That is to say, the materials have the different tension modulus E_t and compression modulus E_c. As shown in the Fig. 1, the bimodulus problem is physically nonlinear (bilinear).

Assuming that the elastic body investigated be continuous deformation, homogeneous, and isotropic, with the difference in the symbol of normal stress, correspondingly, there are different elastic properties. This material has a linear elastic deformation in the random stress state, and satisfies the general law of continual medium mechanics. In other words, basic equations are identical to that of the same modulus theory, and the difference is only reflected in the physical equation.

3. Theoretical analysis and structurual model

As shown in Fig. 2, a pin-ended slender rod with the same modulus remains straight till the axial load is increased to the critical value of F_{cr}. And then the rod will bow. Simultaneously, the neutral axis of the cross-section will coincide with the geometrical center line which divides the cross-section into two parts, the tensile zone and the compressive zone. After taking into account the effect of different moduli in tension and compression, the neutral axis will move to the tensile zone for $E_t > E_c$, while for $E_t < E_c$, the condensable zone, as plotted in Fig. 3. Hence, the initial problem to be addressed is the determination of the position of neutral axis, following which the buckling critical load of the rod can be ascertained.

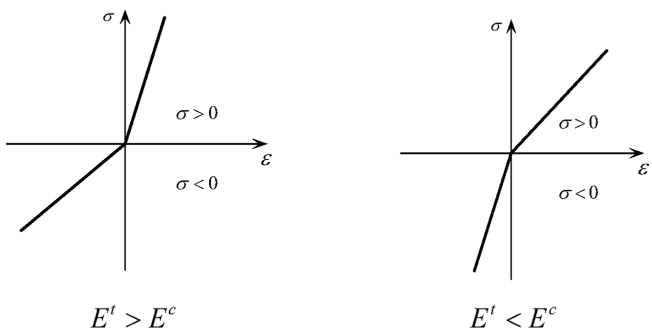

Fig. 1 Constitutive relationship of bimodular materials (bilinear models)

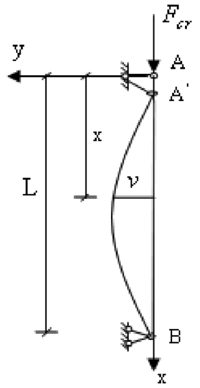

Fig. 2 Buckling of pin-ended slender rod

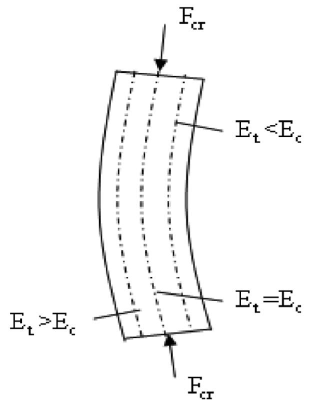

Fig. 3 Neutral axis of bimodular rod under critical state

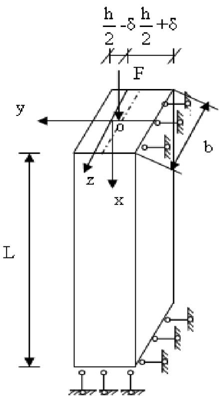

Fig. 4 Structure model

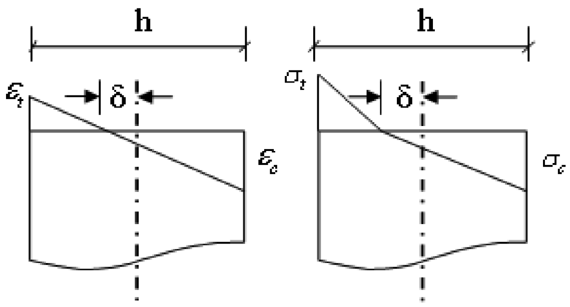

Fig. 5 Distribution of stress and strain in the section

Consider a uniform rod of length L, width b, height h with two ends pin-jointed boundary conditions, ignoring body weight and subjected to axial load F, as displayed in Fig. 4. It should be noted that, as shown in Fig. 4, the neutral axis of the cross-section moves to the tensile zone in the case of $E_t > E_c$. Using the symbol δ (hereinafter referred to as offset) to denote the distance of the neutral axis from the geometrical center line, and for any cross section in the *yoz* plane along x axis, the origin of coordinate will uniformly passes through the neutral axis Fig. 5 depicts the distribution of stress and strain in the section, where ε_c and ε_t represent the compressive strain and the tensile strain which take place on both edges of the cross section in the x direction respectively. Correspondingly, σ_c and σ_t respectively denote stress of tension and compression region on both edges of the section in the x direction.

4. Neutral axis and deflection differential equation

The bending deformation of buckling occurs to the bimodular pin-jointed rod owing to the action of axial load F which reaches the critical value of F_{cr}. As no shear stress applies along the cross section, the neutral layer can be directly determined according to the sign of the normal stress. The deflections of the central axis along from the intial position are identified by v and the deformation still conforms to plane cross-section assumption, that is, the cross section is still plane after deformation, perpendicular to the rod axis, and only makes a relative rotation.

Take a segment dx with its relative rotation $d\theta$ from a rod and the radius of curvature of the neutral layer is ρ, as shown in Fig. 6. The normal strain of a random point whose distance to the coordinate is y can be expressed as

$$\varepsilon_x = \frac{(\rho+y)d\theta-\rho d\theta}{\rho d\theta} = \frac{y}{\rho} = y\frac{d^2v/dx^2}{[1+v'^2]^{3/2}} \tag{1a}$$

Herein, the assumption in the formula of critical buckling load with the same modulus theory for slender rod is still adopted. That is, the deflection curve of the linear elastic rod is smooth and flat, so $v'(x) << 1$, $(1+v'^2)^{3/2} \approx 1$, then we have

$$\varepsilon_x = \frac{(\rho+y)d\theta-\rho d\theta}{\rho d\theta} = \frac{y}{\rho} = y\frac{d^2v}{dx^2} \tag{1b}$$

As it is a phycically bilinear problem, applying a physical equation to the tensile or compressive region gives the normal stress of any point in an arbitrary section

$$\sigma_p = E_t\frac{y}{\rho} = E_ty\frac{d^2v}{dx^2}, \quad \sigma_n = E_c\frac{y}{\rho} = E_cy\frac{d^2v}{dx^2} \tag{2}$$

Where, σ_p, σ_n are the normal stresses of tension and compression zones in the x direction.

It is found that the neutral axis will move to the tensile zone with an offset δ in the case of $E_c/E_t < 1$, therefore the extensinal region height is h_p, and the compressive region height h_n, as shown in Fig. 7. Herein, h_p and h_n are expressed with δ as follows

$$h_p = \frac{h}{2}-\delta \qquad h_n = \frac{h}{2}+\delta \tag{3}$$

The bimodular rod will yield and bend when the axial load acted on the section increase to the critical value F_{cr}, as presented in Fig. 8. Invoking the

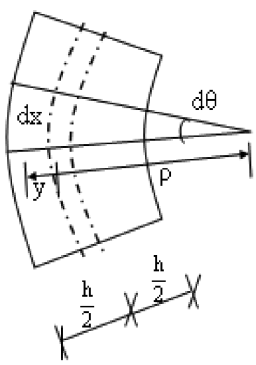

Fig. 6 Structural deformation

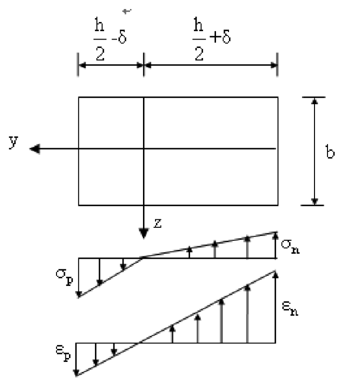

Fig. 7 Schematic cross-section

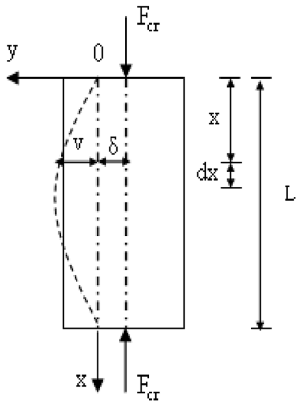

Fig. 8 Buckling of bimodular rod

$$\int_{-h/2-\delta}^{0} \sigma_n b dy + \int_{0}^{h/2-\delta} \sigma_p b dy = F_{cr} \tag{4}$$

Substituting Eq. (2) into Eq. (4) and performing integral operation yields

$$\left[E_t\left(\frac{h}{2}-\delta\right)^2 - E_c\left(\frac{h}{2}+\delta\right)^2\right]\frac{b}{2}\frac{d^2v}{dx^2} = F_{cr} \tag{5}$$

From the above equation, δ can be derived as follows

$$\delta = \frac{(E_t+E_c)h + 2\sqrt{E_tE_ch^2 + \dfrac{2F_{cr}(E_t-E_c)}{bd^2v/dx^2}}}{2(E_t-E_c)} \tag{6}$$

In Eq. (6), δ is referred to as the offset of neutral axis determined from the nonlinear relationship among which *Et* being the tensile modulus, E_c being the compressive modulus, F_{cr} being the critical load and d^2v/dx^2 the curvature. Nevertheless, the critical load F_{cr} is the unkown parameter what we want to acquire. Consequently, we should look for another way to evaluate the critical load for we couldn't obtain it by solving Eq. (5) directly.

According to the Saint-Venant principle, we have

$$\int_{-h/2-\delta}^{0} \sigma_n b y dy + \int_{0}^{h/2-\delta} \sigma_p b y dy = M \tag{7}$$

Combining Eq. (2) with Eq. (7) and integrating gives the bending moment of any cross section written as

$$M = \frac{b}{3}\left[E_c\left(\frac{h}{2}+\delta\right)^3 + E_t\left(\frac{h}{2}-\delta\right)^3\right]\frac{d^2v}{dx^2} \tag{8}$$

On the condition that the bending moment of any section should be equal to the moment of axial load about the deflection of the shifting neutral axis, we get

$$F_{cr}(v+\delta) = M \tag{9}$$

Substituting Eq. (5) and Eq. (8) into Eq. (9), we solve

$$v+\delta=\frac{M}{F_{cr}}=\frac{\frac{b}{3}\left[E_c\left(\frac{h}{2}+\delta\right)^3+E_t\left(\frac{h}{2}-\delta\right)^3\right]\frac{d^2v}{dx^2}}{\frac{b}{2}\left[E_t\left(\frac{h}{2}-\delta\right)^2-E_c\left(\frac{h}{2}+\delta\right)^2\right]\frac{d^2v}{dx^2}} \tag{10}$$

Simplifying Eq. (10), we get

$$v+\delta=\frac{M}{F_{cr}}=\frac{2}{3}\cdot\frac{\frac{E_c}{E_t}\left(\frac{h}{2}+\delta\right)^3+E_t\left(\frac{h}{2}-\delta\right)^3}{\left(\frac{h}{2}-\delta\right)^2-\frac{E_c}{E_t}\left(\frac{h}{2}+\delta\right)^2} \tag{11}$$

Moving the term of δ to the right side of Eq. (11) and simplifying it, the deflection of the central axis for the bimodular rod can be derived as follows

$$v=\frac{1}{3}\cdot\frac{\frac{E_c}{E_t}\left(\frac{h}{2}+\delta\right)^2(h-\delta)+\left(\frac{h}{2}-\delta\right)^2(h+\delta)}{\frac{E_c}{E_t}\left(\frac{h}{2}+\delta\right)^2-\left(\frac{h}{2}-\delta\right)^2} \tag{12}$$

Introducing the following definitions

$$\eta=\frac{v}{h}\qquad\zeta=\frac{\delta}{h} \tag{13}$$

where η represents nondimensional quantity of the offset of the neutral axis and ζ denotes nondimensional quantity of the deflection, into Eq. (12) yield

$$\eta=\frac{v}{h}=\frac{1}{3}\cdot\frac{\frac{E_c}{E_t}\left(\frac{1}{2}+\zeta\right)^2(1-\zeta)+\left(\frac{1}{2}-\zeta\right)^2(1+\zeta)}{\frac{E_c}{E_t}\left(\frac{1}{2}+\zeta\right)^2-\left(\frac{1}{2}-\zeta\right)^2} \tag{14}$$

Eq. (14) presents the evolution of ζ against corresponding η with different value of E_c/E_t. In order to demonstrate the relationship between ζ and η with clarity, within the definition of $E_c/E_t = m$, the variations of ζ against η at various m which vary from 0.2 to 10 are plotted in Fig. 9.

Fig. 9 depicts that the neutral axis gradually shifts from the tensile zone to the compressive zone with the increment of the deflection. When the deflection approaches a certain value (correspondingly η = 7), the offset of the neutral axis tends to decrease with increasing delfection and reaches different constants at various m. This implies that the bearing capacity of the cross section for the bimodular rod no longer increases and approaches a constant (namely the critical load) when the offset of the neutral axis as well as the deflection are extremely close to the limit values, respectively. Table 1 defines the correlation parameters of the bimodular rod in the buckling critical state at different E_c/E_t.

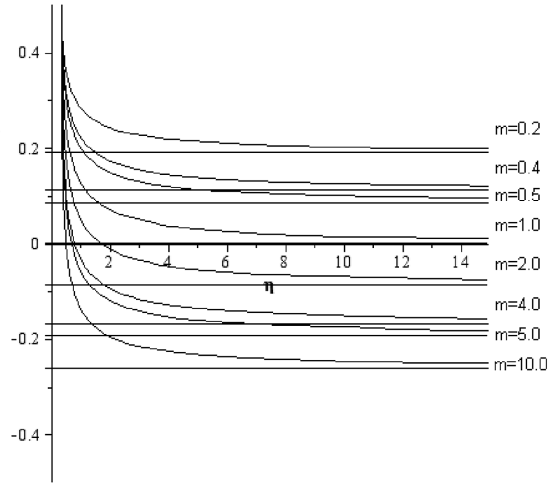

Fig. 9 Relationship between neutral axis and deflection

Table 1 Parameters of bimodular rod with different m in critical state

m (E_c/E_t)	ζ (δ/h)	η (v/h)	$v_{\max}$/m	δ/m
0.20	0.20	7	10*h	0.20*h
0.40	0.12	7	10*h	0.12*h
0.50	0.08	7	11*h	0.08*h
1.00	0.01	7	15*h	0.01*h
2.00	-0.09	7	11*h	-0.09*h
4.00	-0.18	7	11*h	-0.18*h
5.00	-0.20	7	10*h	-0.20*h
10.00	-0.26	7	10*h	-0.26*h

From Table 1, we can see that, in the buckling critical state,with the increment of the ratio of compressive modulus to tensile modulus, the neutral axis moves to the direction which extends the tensile zone (lessen the compressive zone). The offset of neutral axis can be ultimately obtained at various m when the deflection approaches the maximum value. This implies that the bearing capacity of the cross section for the bimodular rod no longer increases and reaches the critical load.

Based on the internal force equilibrium condition, we subsititute Eq. (8) into Eq. (11), and the deflection differential equation of bimodular rod can be achieved as follows

$$\frac{b}{3}\left[E_c\left(\frac{h}{2}+\delta\right)^3+E_t\left(\frac{h}{2}-\delta\right)^3\right]\frac{d^2v}{dx^2}+F_{cr}(v+\delta)=0 \tag{15}$$

Eq. (15) is the buckling deflection differential equation of bimodular slender rod subjected to the axial load. When $E_c = E_t$ and $\delta = 0$, the formula above returns to that of the same modulus theory in classical mechanics.

5. Calculation for the buckling critical load of bimodular slender rod

According to Eq. (15), it is found that the buckling critical load of bimodular slender rod is determined by the tensile modulus, compressive modulus, offset of the neutral axis and the curvature. Owing to the semi-analytical method proposed in this paper, the offset δ of the neutral axis can be achieved. Thus, if the offset δ as a known quantity is introduced to Eq. (15), the general solution of Eq. (15) can be easily written in the following form

$$v = C\sin\left(\frac{\pi x}{L}\right) + D\cos\left(\frac{\pi x}{L}\right) \tag{16}$$

The coefficient of D can be deduced based on the boundary condition of $v|_{x=0} = 0, v|_{x=L} = 0$, and it yields $D = 0$. Hence, Eq. (16) can be rewritten as

$$v = C\sin\left(\frac{\pi x}{L}\right) \tag{17}$$

Eq. (17) is the deflection equation of pin-ended rod, in which the deflection of the rod reaches the maximum C at $x = L/2$.

Differentiating the function v twice, then subsitituting it into Eq. (15), the critical load can be expressed as

$$F_{cr} = \frac{\frac{b}{3}\left(\frac{\pi}{L}\right)^2\left[E_c\left(\frac{h}{2}+\delta\right)^3 + E_t\left(\frac{h}{2}-\delta\right)^3\right]C\sin\left(\frac{\pi x}{L}\right)}{C\sin\left(\frac{\pi x}{L}\right)+\delta} \tag{18}$$

Fig. 9 in the third section shows the process that how the offset of the neutral axis in the buckling critical state and the corresponding maximum delfection C are determined, and the results are listed in Table 1. Substituting the obtained δ and C into Eq. (18), ultimately the buckling critical load F_{cr} of pin-ended bimodular slender rod can be obtained.

6. Example and result

Consider a pin-ended rod of length $L = 1$ m, with rectangular cross section with a dimension of $b \times h = 0.01$ m $\times$ 0.01 m, as shown in Fig. 4. Let us choose different elastic modulus in the following three cases: (1) Keep the average of the two modulus $E = 4000$ MPa unchanged, with the E_c/E_t and E_t/E_c varying between 1 and 10; (2) The tensile modulus E_t remains 1000 MPa, with E_c/E_t varying from 0.1 to 10; (3) The compressive modulus E_c stays the same as 1000 MPa, when E_t/E_c varies in a range with $E_t/E_c = 0.1$~10. The rod is loaded by a concentrated tip load F. The critical buckling load is obtained by using the same modulus theory in classical mechanics, the different modulus theory proposed and the FEM method. To develop a model of the pin-ended rod under buckling analysis, the general purpose finite element program ANSYS was employed in this study. The aforementioned rod has been modeled with *SOLID45*. *SOLID45*, the element which is defined by eight nodes having three degrees of freedom at each node: translation in the nodal x, y, and z directions, is used for the three-dimensional modeling of solid structures. Fig. 10 and Fig. 11

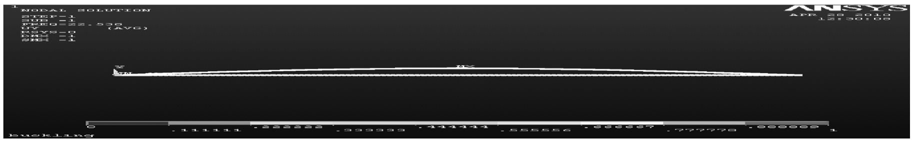

Fig. 10 Buckling deformation of bimodular rod ($E_c = 1600$ MPa, $E_t = 6400$ MPa, $F_{cr} = 23.01$ N)

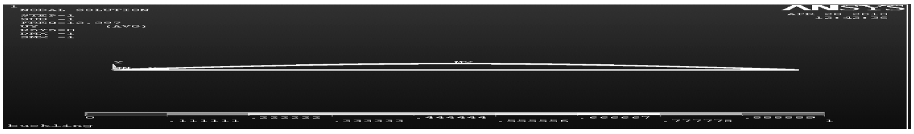

Fig. 11 Buckling deformation of bimodular rod ($E_c = 6400$ MPa, $E_t = 1600$ MPa, $F_{cr} = 23.53$ N)

Table 2 The neutral axis offset and the critical buckling load with the same modulus in classical mechanics

	The extensional modulus E_t/MPa	The compressive modulus E_c/MPa	Neutral axis offset δ/m	Buckling critical load F_{cr}/N
The ratio of two modulus $E_c/E_t = 1.0$	4000	4000	0	32.90
	1000	1000	0	8.22

Table 3 The neutral axis offset and buckling critical load of two methods with unchanged average modulus E

	E_t/MPa	E_c/MPa	E_t/E_c	δ/m	F_{cr}/N (semi-analytcical method)	F_{cr}/N (FEM)	The errors of two methods δF_{cr}(%)
$E = 4000$ MPa	7272.7	727.3	10.0	$0.26h$	13.32	13.81	3.68
	7111.1	888.9	8.0	$0.24h$	15.43	15.75	2.09
	6857.1	1142.9	6.0	$0.22h$	18.41	18.61	1.07
	6400.0	1600.0	4.0	$0.17h$	22.84	23.01	0.69
	5333.3	2666.7	2.0	$0.08h$	29.78	29.85	0.24
	4000.0	4000.0	1.0	$0.01h$	32.89	32.91	0.06
	E_t/MPa	E_c/MPa	E_c/E_t	δ/m	F_{cr}/N (semi-analytical method)	F_{cr}/N (FEM)	The errors of two methods δF_{cr} (%)
	4000.0	4000.0	1.0	$0.01h$	32.89	32.91	0.06
	2000.0	6000.0	3.0	$-0.13h$	26.95	26.59	1.34
	1333.3	6666.7	5.0	$-0.20h$	21.53	20.94	2.74
	1000.0	7000.0	7.0	$-0.23h$	17.92	17.33	3.29
	800.0	7200.0	9.0	$-0.25h$	15.35	14.81	3.52
	727.3	7272.7	10.0	$-0.26h$	14.34	13.81	3.70

present the results modeled by ANSYS, which are compared to those obtained by the other two methods mentioned above. The buckling critical loads, that are computed by the three methods, are tabulated in Tables 2-5 (partial results list only).

Table 4 The neutral axis offset and buckling critical load of two methods with unchanged tensile modulus E_t

	E_c/MPa	E_c/E_t	δ/m	F_{cr}/N (semi-analytical method)	F_{cr}/N (FEM)	The errors of two methods δF_{cr} (%)
$E_t = 1000$ MPa	100	0.1	0.28h	1.83	1.90	3.83
	300	0.3	0.16h	4.03	4.12	2.23
	600	0.6	0.07h	6.21	6.27	0.97
	800	0.8	0.03h	7.30	7.34	0.55
	1000	1.0	0.01h	8.22	8.23	0.12
	3000	3.0	-0.14h	13.48	13.23	1.85
	6000	6.0	-0.22h	17.10	16.59	2.98
	8000	8.0	-0.24h	18.60	17.96	3.44
	10000	10.0	-0.28h	19.72	18.99	3.70

Table 5 The neutral axis offset and buckling critical load of two methods with unchanged compressive modulus E_c

	E_t/MPa	E_t/E_c	δ/m	F_{cr}/N (semi-analytical method)	F_{cr}/N (FEM)	The error of two methods δF_{cr} (%)
$E_c = 1000$ MPa	100	0.1	-0.26h	1.97	2.04	3.71
	300	0.3	-0.15h	4.21	4.30	2.08
	600	0.6	-0.07h	6.33	6.39	0.97
	800	0.8	-0.03h	7.37	7.40	0.44
	1000	1.0	0.01h	8.22	8.23	0.12
	3000	3.0	0.13h	12.98	13.21	1.78
	6000	6.0	0.22h	16.11	16.69	3.16
	8000	8.0	0.24h	17.36	17.96	3.45
	10000	10.0	0.26h	18.31	18.96	3.55

7. Test and result

For a further validation of the proposed semi-analytical method, the experiments are designed to perform tests on the materials mechanical properties of graphite (MSL82) specimens by the electronic universal testing machine (WDW-E100) and the electronic universal testing machine (CMT5306). The tests include the following: 1) uniaxial compressive test; 2) uniaxial tensile test; 3) buckling test.

7.1 Material mechanical properties tests

In the uniaxial tensile test, four specimens are made of graphite (MSL82). The size of the cylindrical specimens are Radius = 10 mm and Height = 50 mm. While in the uniaxial compressive

Table 6 Test results on the mechanical properties of graphite (MSL82)

Specimen number	Ultimate tensile strength (MPa)	Ultimate compressive strength (MPa)	Tensile elastic modulus (GPa)	Compressive elastic modulus (GPa)	E_c/E_t
1	26.70	72.76	8.62	11.90	1.38
2	30.70	68.37	8.59	12.32	1.43
3	28.77	65.02	8.84	12.58	1.42
4	26.70	70.95	8.73	12.26	1.40
Mean	28.22	69.28	8.70	12.27	1.41

test, the size of the four cylindrical specimens are Radius = 10 mm and Height = 200 mm. The contents of these texts contain ultimate tensile strength, ultimate compressive strength, tensile elastic modulus, compressive elastic modulus and calculate E_c/E_t. The test results are tabulated in Table 6.

7.2 Buckling tests

The buckling stability tests are conducted in the electronic universal testing machine (WDW-E100) which is shown in Fig. 12. The configuration and dimensions (500 mm × 30 mm × 30 mm) of graphite (MSL82) specimens are shown in Fig. 13 and Fig. 14. Test results are tabulated in Table 7 and plotted in Fig. 15.

Fig. 12 Testing device and loading mode

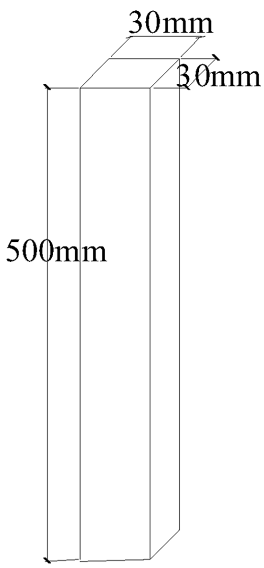

Fig. 13 Specimen size

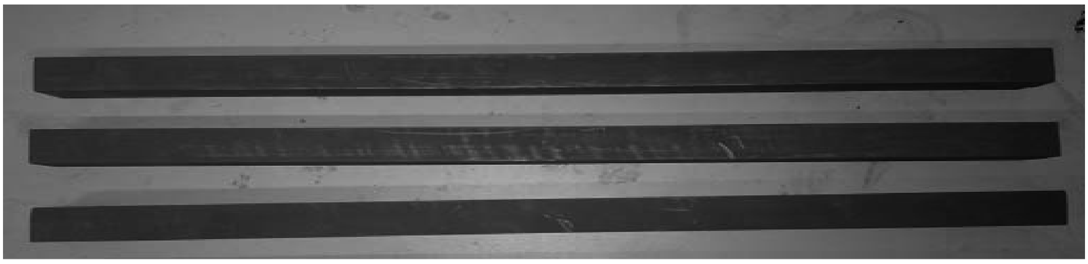

(a) Specimen before tests

(b) Specimen after tests

Fig. 14 Specimens of graphite materials (MSL82)

Table 7 Buckling tests results and semi-analytical solutions

Specimen number	1	2	3	Mean	Semi-analytical solutions	The error δF_{cr} (%)
Buckling critical load (kN)	34.58	25.38	34.78	31.58	28.51	9.7

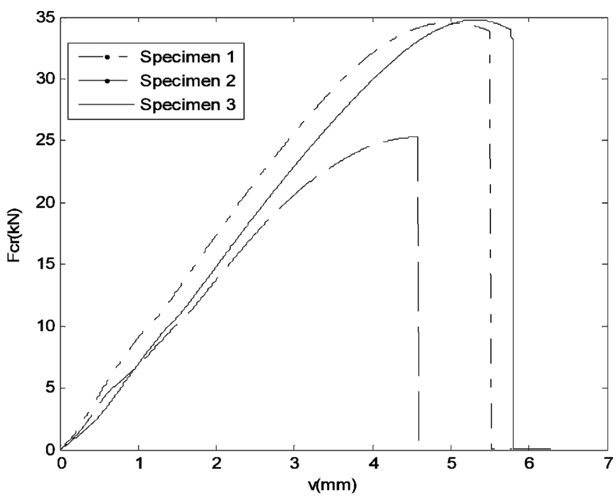

Fig. 15 The diagram of the tests

8. Discussion

8.1 Model verification and error analysis

The solutions(see Tables 3-5) obtained by the semi-analytical method for the same modulus problem are in very good agreement with those obtained by the analytical solutions (see Table 2) of the same modulus theory in classical mechanics. The error amount is around 0.01%. Thus, the analytical solutions by using different modulus can return to the results of the same modulus theory in classical mechanics. Besides, Fig. 16 shows a good coincidence between the semi-analytical solutions and the results of finite element analysis. As is depicted in Fig. 17, the maximum error is 3.8%. Moreover, comparing the semi-analytical solutions with the test results (see Tables 6, 7) for the graphite material (MSL82) with E_c/E_t of 1.41, there is a good agreement with a difference within 9.7% between the two results. Thus, the semi-analytical method developed in this paper is reliable.

8.2 The difference between different modulus and same modulus problems

When different moduli are introduced, regular variations occur in the neutral axis of the bimodular rod, as shown in Fig. 18. With the increase of E_c/E_t, the neutral axis gradually moves from the tensile zone to the compressive zone. In other words, the height of tension region tends to increase with increasing E_c/E_t, and vice versa.

For the materials with the average modulus E equalling to 4000 MPa, when E_c as well as E_t varies (see Fig. 16 in which the logarithmic coordinate is chosen as the transverse axis), comparing to the rod with the same modulus, the critical buckling load is smaller whether E_c/E_t increases or declines. Moreover, the critical buckling load is more sensitive to the deduction of E_c (see Fig. 19).

When introducing the different moduli, one of which remains the same at 1000 MPa, and the addition reflected only in the other modulus, then the enhancement of F_{cr} characterizes regionally, as shown in Figs. 20, 21 (the logarithmic coordinate is chosen as the transverse axis). That is, F_{cr} has a notable change from 1.83 N to 8.22 N (3.5 times of the original value) when E_c increases by

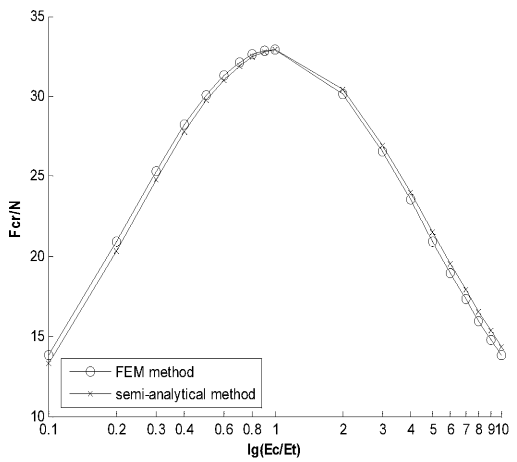

Fig. 16 The results of the two methods with unchanged average modulus $E = 4000$ MPa

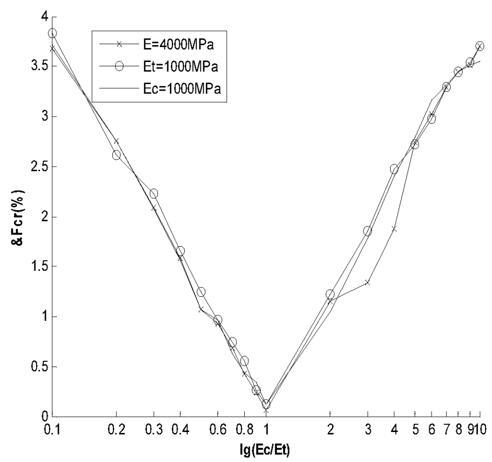

Fig. 17 The errors of the two methods with different modulus

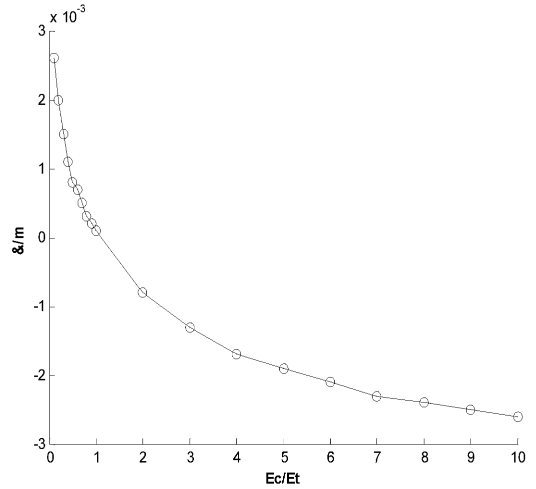

Fig. 18 The variation of the neutral axis offset against the ratio of two modulus

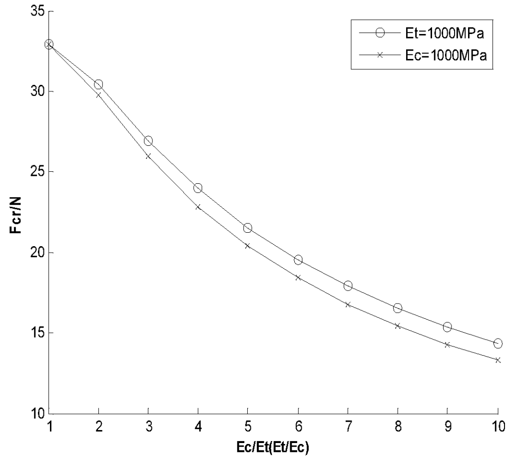

Fig. 19 The variation of critical buckling loads against E_c/E_t (E_t/E_c) when the average modulus equalling 4000 MPa

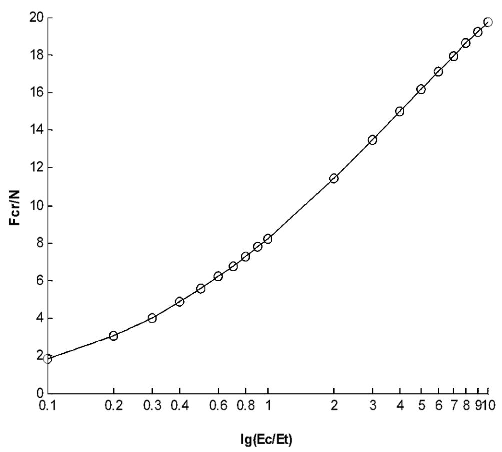

Fig. 20 The variation of critical buckling load against E_c/E_t when E_t = 1000 MPa

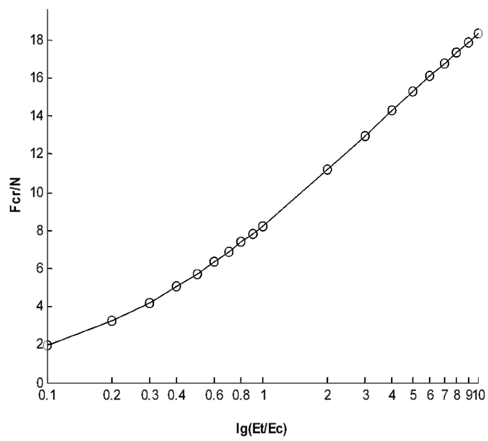

Fig. 21 The variation of critical buckling load against E_t/E_c when E_c = 1000 MPa

10 times of 100 MPa. However, as E_c varies from 1000 MPa to 10000 MPa (increases by 10 times as well), F_{cr} enhances slowly (only increases by 1.4 times). In addition, a similar phenomenon will happen with the variation of E_t (see Fig. 21).

When remaining E_c (or E_t) unchanged, E_c and E_t have different regional influence on F_{cr}. As is depicted in Fig. 22, in the case of E_c/E_t (E_t/E_c) < 2, the curve about the variation of F_{cr} against E_c is in coincidence with that about the evolution of F_{cr} against E_t. That is to say, to increase E_c or E_t has almost the same impact on the improvement of F_{cr}. However, when E_c/E_t (E_t/E_c) > 2, the difference between the two curves will enlarge and the curve about the variation of F_{cr} against E_c is steeper. It implies that the increase of E_c has a more remarkable effect on enhancing F_{cr}.

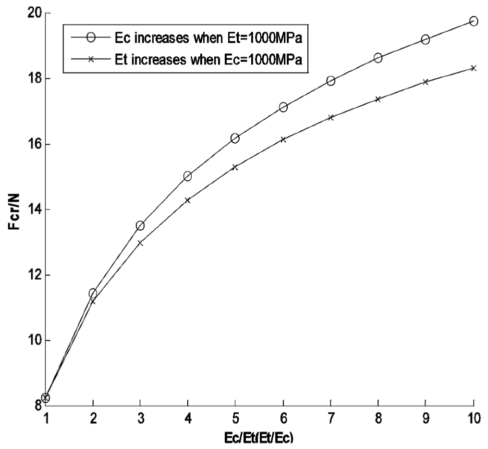

Fig. 22 The variation of critical buckling load against E_c/E_t (E_t/E_c)

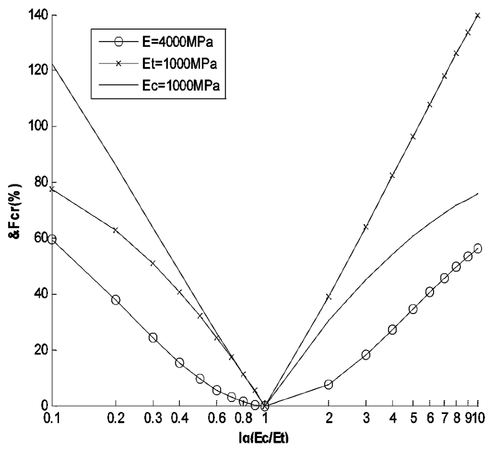

Fig. 23 The errors between the same modulus and different modulus methods versus E_c/E_t in three cases

For the aforementioned materials with different moduli in the three cases, when comparing with the results of the same modulus problem, the difference between which and the semi-analytical solutions will be wider with the continuous increase or decrease of the ratio of E_c/E_t. Particularly, when E_c increases to 5 times of E_t, the results errors of two methods have reached 30%, 60%, 80%, respectively (see Fig. 23).

9. Conclusions

In this study, the results of E_c/E_t (E_t/E_c) = 0.1-10 are listed. It is shown that the analytical solutions by using different modulus can return to the result of the same modulus theory in classical mechanics. And there is a good agreement between the results of the introduced approach and the finite element method and the buckling tests. Thus, the method proposed in this paper is effective for buckling analysis of bimodular rod. Some conclusions are drawn as follows:

(1) When the total of the two modulus stays the same, compared with the same modulus problem, the critical buckling load decreases with the increasing difference of different modulus. This is because of the uneven stiffness caused by the bimodular difference of the two modulus. This uneven stiffness will induce a weakening effect on the resistance of buckling. Consequently, stability analysis of bimodular structures is extremely important.

(2) As only one modulus increases with the other unchanged, the enhancement of critical buckling load reflects regionally. In the case of E_c/E_t (E_t/E_c) = 0.1-1, the buckling critical load increases fast. This indicates that, owing to the increase of the modulus, the global section stiffness increases and gradually becomes even, which accounts for a notable improvement for the rod to resist buckling. In the case of E_c/E_t (E_t/E_c) = 1-10, the critical load increases slowly. Because the gap of the two modulus widens, which causes the stiffness uneven. So the ability for the rod to withsand buckling improves relatively slowly.

(3) Compared with the results of the same modulus problem, the critical load increases

remarkably due to the increment of Ec. Accordingly, for the structure with different modulus, we can improve structure stability by increasing the compressive modulus, so that the structure can be optimized.

(4) Most materials applied in the engineering have the ratio of different modulus within a range of $E_c/E_t = 1\text{-}5$. For $E_c/E_t = 5$, the error of the results between the different modulus methods and the same modulus methods has reached approximately 78%. Therefore, for the structure with great difference between tension modulus and compression modulus, it should be calculated and analyzed by the different modulus theory instead of the same modulus theory.

By using the method proposed in this paper to determine the neutral axis, the cost of computation may be lower than that of the multi-iterations methods because of the advantage of improved stability and faster convergence. The method is also simple and straightforward. Hence, this methodology could be very valuable in solving the buckling problem of bimodular rods or bimodular structures.

References

Ambartsumyan, S.A. (1986), *Elasticity Theory of Different Modulus*, Eds. W. Ruifeng and Z. Yunzhen, Railway Press, Beijing, China.

Barak, M.M., Currey, J.D., Weiner, S. and Shahar, R. (2009), “Are tensile and compressive Young’s moduli of compact bone different”, *J. Mech. Behav. Bimed. Mat.*, **2**(1), 51-60.

Bert, C.W. (1977), “Models for fibrous composites with different properties in tension and compression”, *J. Eng. Mat. Tech.*, **99**(4), 344-349.

Bert, C.W. and Ko, C.L. (1985), “Buckling of columns constructed of bimodular materials”, *Int. J. Eng. Sci.*, **23**(6), 641-657.

Bertoldi, K., Bigoni, D. and Drugan, W.J. (2008), “An orthotropic and bimodular elastic material”, *Compos. Sci. Tech.*, **68**, 1363-1375.

Bruno, D., Lato, S. and Sacco, E. (1994), “Nonlinear analysis of bimodular composite plates under compression”, *Comput. Mech.*, **14**, 28-37.

Cai, L. and Yu, H. (2009), “Constitutive relation of elastic materials with different elastic moduli in tension and compression”, *J. Xi’an Univ. Sci. Tech.*, **29**(1), 17-21.

Destrade, M., Gilchrist, M.D., Motherway, J.A. and Murphy, J.G. (2009), “Bimodular rubber buckles early in bending”, *Mater. Mech.*, **42**(4), 469-476.

He, X.T. (2007), “Applying the equivalent section method to solve beam subjected to lateral force and bend-compression column with different moduli”, *Int. J. Mech. Sci.*, **49**, 919-924.

He, X.T., Zheng, Z.L. and Sun, J.Y. (2009), “Convergence analysis of a finite element method based on different moduli in tension and compression”, *Int. J. Solids Struct.*, **46**(20), 3734-3740.

Jones, R.M. (1977), “Stress-strain relations for materials with different moduli in tension and compression”, *Am. Inst. Aeron. Astron.*, **15**(1), 16-23.

Klisch, S.M. (2006), “A bimodular theory for finite deformations: comparison of orthotropic second-order and exponential stress constitutive equations for articular cartilage”, *Bimomech. Model. Mechanobio.*, **5**(2), 90-101.

Leal, A. (2009), “Compressive strength analysis for high performance fibers with different modulus in tension and compression”, *J. Compos. Mater.*, **43**(6), 661-674.

Lan, T., Lin, P.D. and Chen, L.W. (2003), “Thermal buckling of bimodular sandwich beams”, *Compos. Struct.*, **25**, 345-352.

Patel, B.P. (2004), “Thermo-flexural analysis of thick laminates of bimodulus composite materials”, *Compos. Struct.*, **63**(1), 11-20.

Qu, C. (2009), “Deformation of geocell with different tensile and compressive modulus”, *Elec. J. Geotech. Eng.*, **14**, 1-14.

Raffaele, Z. and Fabrizio, G. (2001), “Damage evolution in bimodular laminated composites under cyclic

loading", *Compos. Struct.*, **53**(4), 381-402.
Tseng, Y.P. and Lee, C.T. (1995), "Bending analysis of bimodular laminates using a higher-order finite strip method", *Compos. Struct.*, **30**(3), 341-350.
Tseng, Y.P. and Jiang, Y.C. (1998), "Stress analysis of bimodular laminates using hybrid stress plate element", *Int. J. Solids Struct.*, **35**(17), 2025-2028.
Yang, H. and Zhu, Y. (2006), "Solving elasticity problems with bi-modulus via a smoothing technique", *Chinese J. Comput. Mech.*, **23**(1), 19-23.
Yang, H. and Xu, M. (2009), "Solving inverse bimodular problems via artificial neutral network", *Inverse Pro. Sci. Eng.*, **17**(8), 999-1017.
Yao, W.J., Zhang, C. and Jiang, X. (2006), "Nonlinear mechanical behavior of combined members with different moduli", *Int. J. Nonlin. Sci. Numer. Simul.*, **7**(2), 233-238.
Yao, W.J. and Ye, Z. (2004), "Analytical solution of bending-compression column using different tension-compression modulus", *J. Appl. Math. Mech.*, **25**(9), 901-909.
Yao, W.J. and Ye, Z. (2004), "Analytical solution for bending beam subject to later force with different modulus", *J. Appl. Math. Mech.*, **25**(10), 1014-1022.
Yao, W.J. and Ye, Z. (2004), "The analytical and numerical solution of retaining wall based on elastic theory of different modulus", *J. Shanghai Jiaotong Univ.*, **38**(6), 1022-1027.
Yao, W.J. and Ye, Z. (2006), "Internal forces for statically indeterminate structures having different moduli in tension and compression", *J. Eng. Mech.-ASCE*, **132**(7), 739-746.
Yao, W.J. and Ye, Z. (2005), "Analytical method and the numerical model of temperature stress for the structure with different modulus", *J. Mech. Strength*, **27**(6), 808-814.
Ye, Z.M. (1997), "A new finite element formulation for planar elastic deformation", *Int. J. Numer. Meth. Eng.*, **14**(40), 2579-2592.

Notations

The following are symbols used in this paper:

E_t	: the tensile modulus;
E_c	: the compressive modulus;
F_{cr}	: critical buckling load;
δ	: neutral axis offset;
v	: deflection at point x;
ρ	: radius of curvature;
σ_p	: normal stress in tension area;
σ_n	: normal stress in compression area;
h_p	: the height of tension area;
h_n	: the height of compression area;
d^2v/dx^2	: the curvature;
M	: bending moment of any section;
η	: nondimensional quantity of the neutral axis offset;
ζ	: nondimensional quantity of the deflection;
m	: the ratio of E_c to E_t;
$v_{\max}$	: maximum deflection;
E	: the average modulus;
δF_{cr}	: errors of critical buckling load.